UNCECOMP 2015
1st ECCOMAS Thematic Conference on
International Conference on Uncertainty Quantification in
Computational Sciences and Engineering
M. Papadrakakis, V. Papadopoulos, G. Stefanou (eds.)
Crete Island, Greece, 25–27 May 2015

DESIGN CONSIDERATION OF LARGE-DISPLACEMENT RF MEMS TUNERS UNDER FABRICATION UNCERTAINTIES

Juan Zeng and Dimitrios Peroulis

School of Electrical and Computer Engineering, Birck Nanotechnology Center,
Purdue University, West Lafayette, Indiana, U.S.A
e-mail: zengj@purdue.edu, dperouli @purdue.edu

Keywords: RF MEMS Tuners, Micro-Corrugated Diaphragm, Large-Displacement, Fabrication Uncertainty, Uncertainty Quantification.

Abstract. *RF MEMS capacitive tuners based on micro-corrugated diaphragms in tunable cavity resonators/filters demand for large tuning displacements and low tuning voltages. The tuning characteristics are subjected to fabrication uncertainties of residual stress and corrugation dimensions of the diaphragm. We discuss the design consideration of large-displacement low-voltage diaphragms for reducing the effects of fabrication uncertainties by proper geometric design of the corrugations through batch-mode FEM modeling. Uncertainty quantification is performed to analyze variations of the tuning range and actuation voltage of the capacitive MEMS tuner under fabrication uncertainties.*

1 INTRODUCTION

Widely tunable filters with low insertion loss are essential components in realizing reconfigurable RF-front ends. Evanescent-mode cavity resonators/filters have been successfully demonstrated recently with advantages of wide tuning range, high quality factor, small size, and high power handling capability [1-2]. Fig. 1(a) shows the side view of an evanescent-mode cavity resonator schematically. The conductor-walled cylinder cavity is loaded by a conductive post that serves as an effective shunt capacitor whose capacitance is determined by the gap between the post and the ceiling diaphragm. The resonant frequency is determined by the equivalent capacitance and inductance. Therefore, frequency tuning can be achieved by a diaphragm tuner which can be used to change the gap between the post and the diaphragm. To achieve a large tuning deflection with a reasonably low actuation voltage, MEMS capacitive tuners based on micro-corrugated diaphragms have been employed [3-4]. The corrugated structure elongates the profile length in the radial direction which effectively reduces the stretching stiffness in the radial direction due to residual stress and large displacements, and therefore, significantly reduces the actuation voltage at large displacements [5].

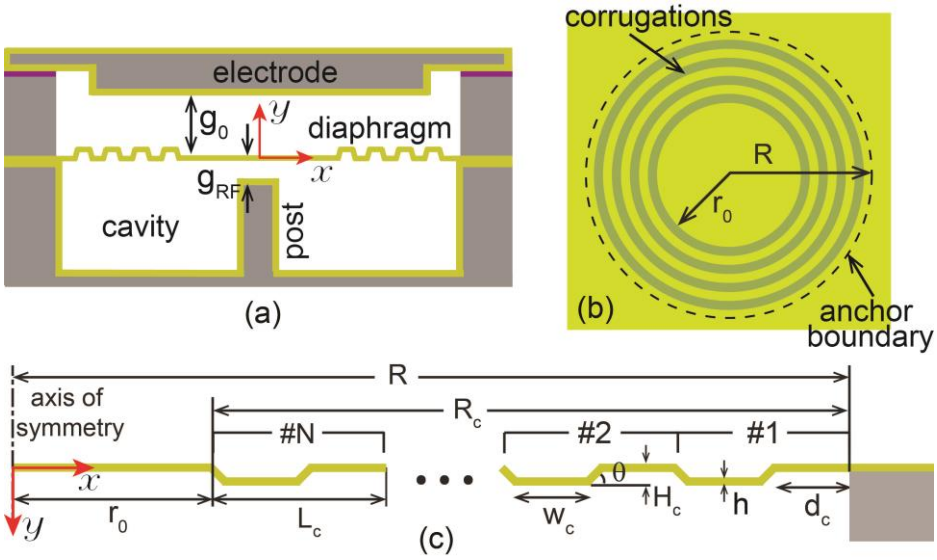

Figure 1: (a) Side view of a tunable cavity resonator, (b) top view and (c) side view of a micro-corrugated diaphragm.

The tuning characteristics are subjected to fabrication uncertainties which cause wafer-to-wafer or even device-to-device variations of residual stress and corrugation dimensions of the diaphragm. We will discuss the design consideration of large-displacement diaphragms for minimizing the effects of fabrication uncertainties.

2 CAPACITIVE TUNER MODELING

2.1 Diaphragm stiffness

For diaphragms designed to operate in the large deflection regime, both linear and nonlinear effects need to be investigated. In the case of small deflections, bending stiffness dominates and the load-deflection behavior can be described by a linear stiffness coefficient k_1. As deflection increases, the stretching-induced stress of the diaphragm causes the nonlinearity in the large deflection regime and therefore, a nonlinear stiffness coefficient k_3 is introduced to account for this nonlinearity. In general, for a diaphragm with a radius R and under a uniform-

ly distributed pressure P, the load-deflection behavior can be approximated by the following relationship [5]:

$$F_m = k_1(w - w_0) + k_3(w - w_0)^3 \quad (1)$$

where $F = \pi R^2 P$ is the total loading force on the diaphragm, w is the center displacement of the diaphragm, and w_0 is the residual-stress-induced initial center deflection. The stiffness coefficients k_1 and k_3 are functions of the diaphragm's geometric and material properties. The in-plane residual stress adds resistance to bending, and therefore, changes the linear stiffness coefficient k_1.

2.2 FEM modeling for diaphragm stiffness

Due to the geometric complexity of corrugated diaphragms, only limited analytical models have been proposed for the prediction of the stiffness with respect to geometric parameters. Therefore, FEM simulations are performed using ANSYS Parametric Design Language (APDL) [7]. The script-based simulation allows ANSYS program to be linked with MATLAB [8] program for systematically changing the geometric parameters of corrugated diaphragms. In this way, the parametric study can be performed efficiently to study the relationship between the diaphragm stiffness and the corrugation parameters. In order to reduce the computation time, the axisymmetry of the diaphragm is utilized by choosing a higher order 2-D, 8-node element PLANE183 with the axisymmetric option activated. In the simulations, only the trapezoidal corrugations are considered as shown in Fig. 1(c). Appropriate boundary conditions are assigned: the surface where the diaphragm attached to the substrate at the outer rim edge of the diaphragm is fixed in both horizontal direction (x-axis) and vertical direction (y-axis). The geometric and material properties assumed in the simulations are listed in Table 1. The stiffness coefficients can be extracted by fitting (1) to the simulated load-deflection curves.

	Parameter	Value
Geometric Attributes	Radius R	900 μm
	Thickness h	1 μm
	Corrugation Wavelength L_c	100 μm
	Corrugation Sidewall Angle θ	45 °
	Corrugation width w_c	$\frac{1}{2}\left(L_c - 2H_c / \tan\theta\right)$
	Corrugation distance d_c	$\frac{1}{2}\left(L_c - 2H_c / \tan\theta\right)$
Material Properties	Young's Modulus E	57 GPa
	Poisson's ratio ν	0.42

Table 1: Dimensions and material properties used in FEM simulations for micro-corrugated diaphragms.

2.3 Electrostatic tuning of diaphragms with nonlinearity

The pull-in instability of electrostatic actuation of the capacitive MEMS tuner dictates that the diaphragm cannot be continuously tuned through the entire gap between the diaphragm and bias electrode. The tuning range of the MEMS tuner is determined by the maximum displacement (w_m) the diaphragm travels before pull-in occurs. When the displacement of the diaphragm increases to w_m, the restoring force cannot balance the electrostatic force and the

pull-in phenomenon occurs. When calculating the pull-in voltage (V_{pi}) and tuning range of MEMS tuners, both the linear and nonlinear stiffness of the diaphragm are considered. With the mechanical restoring force modeled by (1) and the electrostatic force modeled by using a parallel plate capacitance model, the pull-in voltage (V_{pi}) and tuning range can be calculated. When the nonlinear behavior of the diaphragm is dominant ($k_3 >> k_1$), $w_m/g_0 \rightarrow 3/5$; and when the linear behavior is dominant ($k_3 << k_1$), $w_m/g_0 \rightarrow 1/3$.

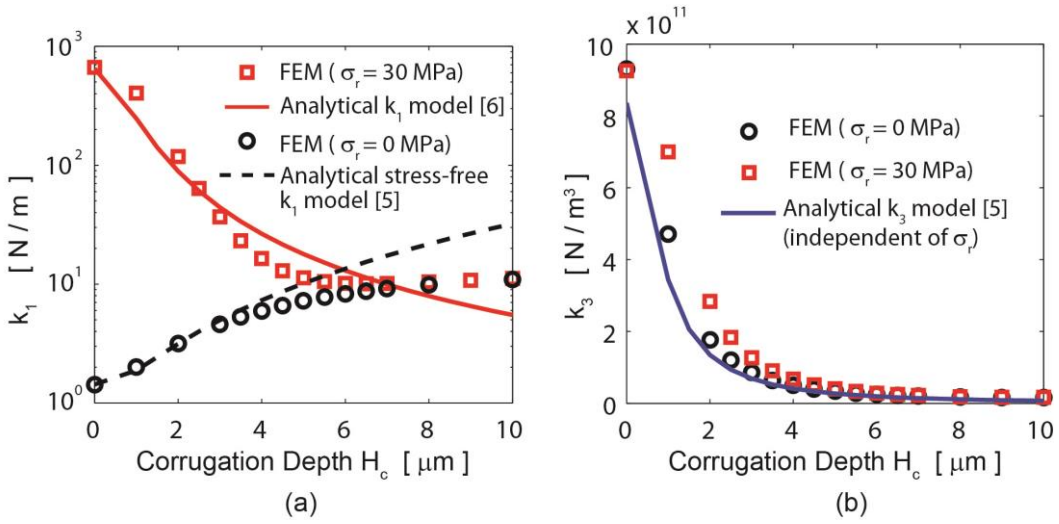

Figure 2: (a) Linear stiffness coefficient k_1 and (b) nonlinear stiffness coefficient k_3 versus corrugation depth H_c. (The geometric and material properties are listed in Table 1, number of corrugations N_c = 4)

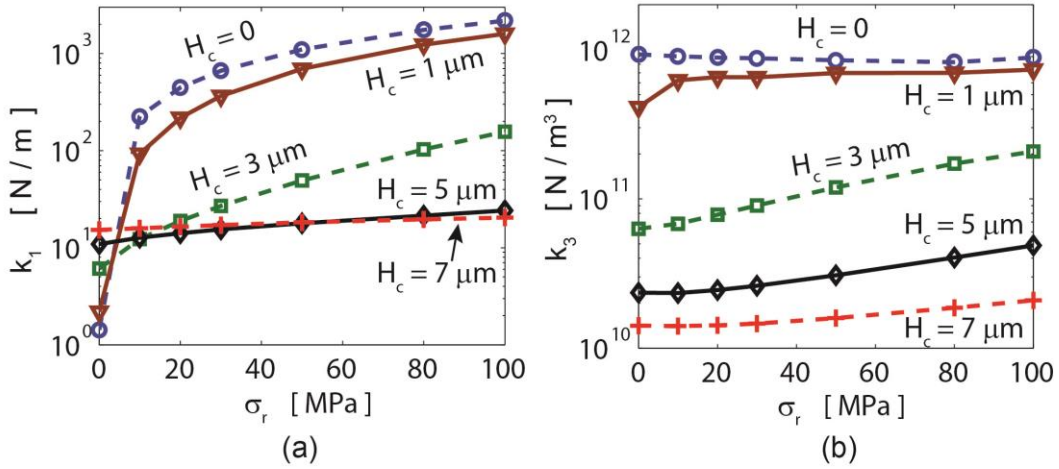

Figure 3: Linear stiffness coefficient k_1 and (b) nonlinear stiffness coefficient k_3 versus residual stress σ_r at different corrugation depth H_c.

3 PARAMETRIC STUDY FOR DESIGN OPTIMIZATION

3.1 Parametric study

A parametric study of the micro-corrugated diaphragm is performed to investigate the dependence of diaphragm stiffness on residual stress and corrugation dimensions, which provides design guidelines for low-voltage, high tuning range capacitive MEMS tuners with considerations of the fabrication uncertainties.

Fig. 2 shows the extracted stiffness coefficients as a function of the corrugation depth H_c, and the comparison between the FEM results and the analytical models in [5] and [6]. In a

stress-free diaphragm, the linear stiffness increases with the increase of corrugation depth. With the presence of residual stress σ_r, an optimal value of H_c corresponds to a minimum linear stiffness k_1. The nonlinear stiffness shows a less significant dependence on the residual stress and decreases with the increase of corrugation depth.

The dependence of the diaphragm stiffness on residual stress is illustrated in Fig. 3. It is evident that a larger corrugation depth can reduce the dependence of the diaphragm stiffness (especially the linear stiffness) on the variation of the residual stress. The dependence of k_1 on σ_r is effectively alleviated by corrugations with $H_c \geq 5$ μm (Fig. 3(a)). k_3 shows a weak dependence on residual stress and it decreases greatly with the increase of the corrugation depth H_c (Fig. 3(b)).

3.2 Tradeoff between tuning range and actuation voltage

The tuning range and tuning voltage of the tuner can be determined once the stiffness coefficients k_1 and k_3 are extracted as stated in Section 2.3. The parametric study shows that the corrugation depth H_c and the corrugation range R_c are the two most important geometric parameters of the corrugations in determining the stiffness of corrugated diaphragms and consequently the pull-in voltage and tuning range. Fig. 4 shows the pull-in voltage and tuning range versus H_c and R_c assuming a residual stress of σ_r = 30 MPa, and an initial DC gap of g_0 = 35 μm.

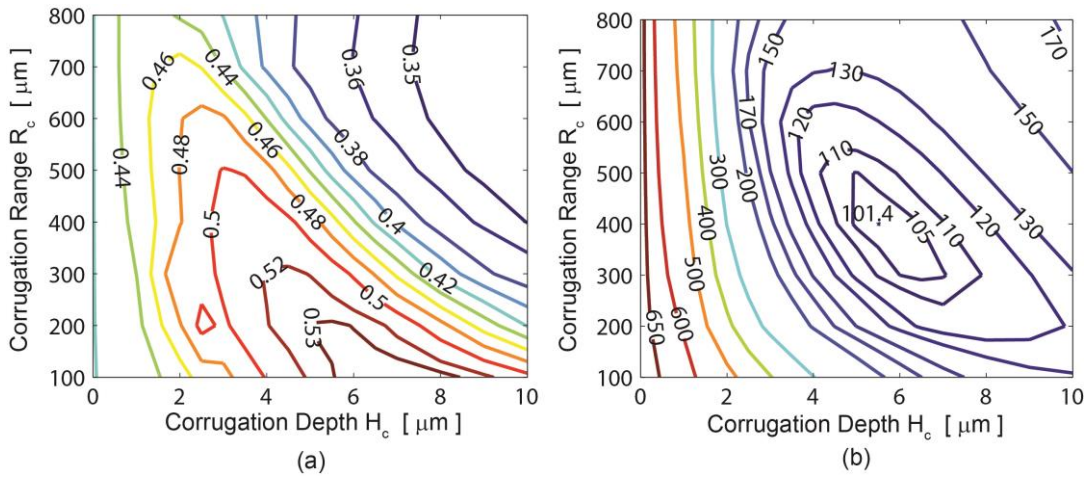

Figure 4: (a) tuning range and (b) actuation voltage for a 12-μm tuning displacement versus R_c and H_c (g_0 = 35 μm, σ_r = 30 MPa).

It is clear that there is a tradeoff between the pull-in voltage and tuning range. We cannot simultaneously achieve the minimum pull-in voltage and the maximum tuning range. The diaphragms are usually tuned below the pull-in voltage to avoid contact degradation. Therefore, the corrugation design should meet the minimum requirement of tuning range. To achieve a tuning displacement of 12 μm with a 4-μm margin to pull-in, the tuning range should be > 0.45. The actuation voltage at the maximum tuning displacement of 12 μm can be minimized by choosing H_c = 5.5 μm and R_c = 400 μm.

3.3 Consideration of fabrication uncertainties

The fabrication uncertainties which cause variations of residual stress and corrugation dimensions of the diaphragm are unavoidable and cause the variations of the tuning characteristics. Therefore, attentions should be paid to minimize the effects of the fabrication uncertainties.

As shown in Fig. 2, for σ_r = 30 ± 10 MPa, the variation of the stiffness coefficients k_1 and k_3 are < 8% for H_c > 5 µm. Therefore, a large corrugation range is desirable to minimize the variations caused by the uncertainty of residual stress. When the actuation voltage is minimized by choosing H_c = 5.5 µm and R_c = 400 µm, the variations of the tuning voltage with respect to the changes of the both H_c and R_c is minimal (Fig. 4) , and the requirement of the tuning range > 0.45 is satisfied at the same time. Therefore, this geometric design is chosen with the consideration of the design requirements and the fabrication uncertainties.

4 UNCERTAINTY QUANTIFICATION

We consider two fabrication uncertainties which are the most significant in causing the variation of the tuning range and the actuation voltage: the residual stress σ_r and the corrugation depth H_c.

4.1 Sample generation for Monte Carlo simulations

The Monte Carlo approach is used to find the output probability density function (PDF) assuming normal distributions of the input parameters σ_r and H_c due to fabrication uncertainty. We assume that the corrugation depth H_c has a mean value of 5.5 µm with a standard deviation (STD) of 0.25 µm, and the residual stress is 30 MPa with a STD of 5 MPa. The normally distributed pseudorandom sampling data are generated by using the randn Matlab function. Fig. 5 shows the 800 sample points in the plane of H_c and σ_r. The PDF of the corrugation depth H_c and the residual stress σ_r are plotted in Fig. 6 with the mean value and STD of the normally distributed pseudorandom sampling sets indicated in the plots.

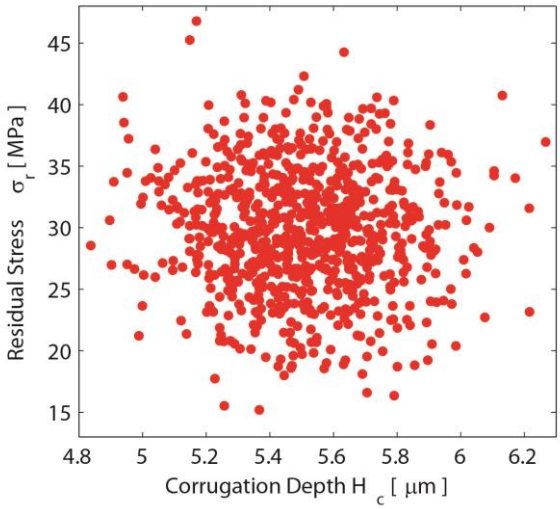

Figure 5: 800 sample points in the plane of H_c and σ_r assuming normal distributions.

4.2 Variation of tuning characteristics due to fabrication uncertainties

The diaphragm with H_c = 5.5 µm and R_c = 400 µm is simulated for each sample points shown in Fig. 5. The results of the tuning range and the actuation voltage also follow nearly normal distributions with small skewnesses as shown in Fig. 7.

The tuning range has a mean value of 0.468 with a STD of 0.014, and the actuation voltage at 12 µm is 101.4 V with a STD of 4.8 V. Therefore, with a 95% confidence level, the tuning range is between 0.440 and 0.496 (a variation of ± 5.9%), and the actuation voltage varies between 91.8 V and 111.0 V (a variation of ± 9.4%). It is worth noticing that the actuation volt-

age always increases no matter the corrugation depth H_c increases or decreases from 5.5 μm as shown in Fig. 4(b). With σ_r = 30 MPa and a variation of $\Delta H_c = \pm 0.5$ μm, the maxim actuation voltage variation is 2.4 V. Therefore, the variation of the actuation voltage due to the uncertainty of the residual stress is more dominant over that due to the uncertainty of the corrugation depth.

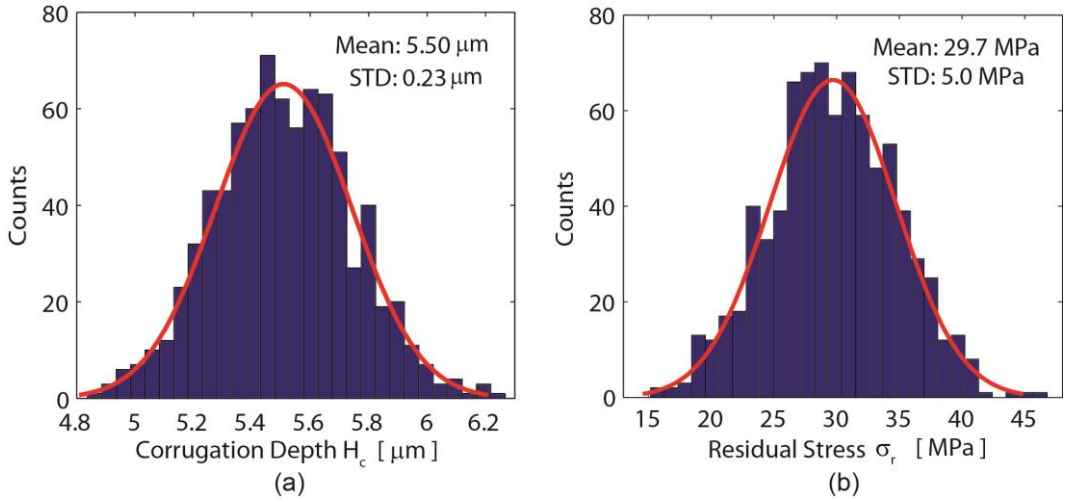

Figure 6: The PDF of 800 sample points of (a) the corrugation depth H_c, and (b) the residual stress σ_r assuming normal distributions.

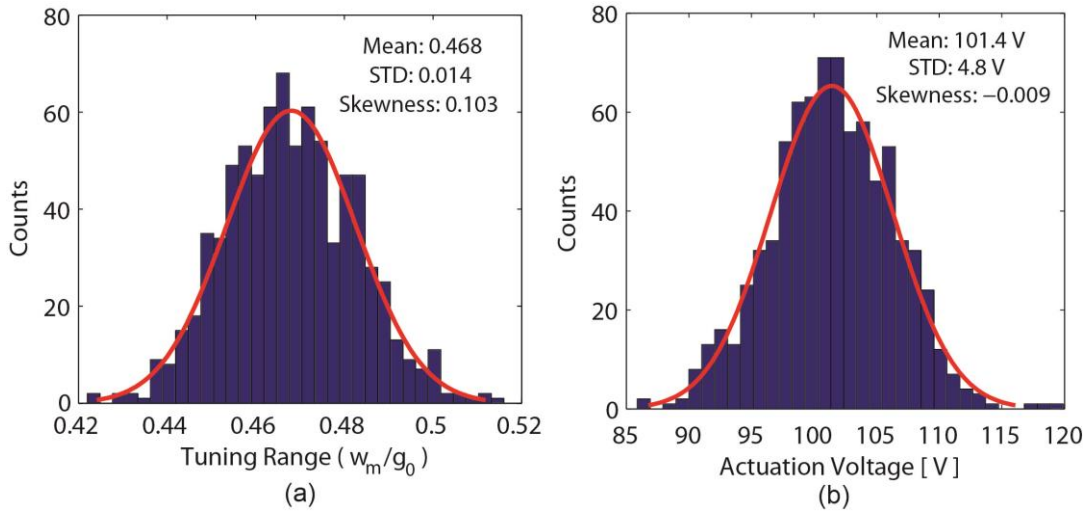

Figure 7: The PDF of (a) the tuning range, and (b) the actuation voltage at a 12-μm tuning displacement due to the fabrication uncertainties of H_c *and* σ_r shown in Fig. 5.

5 CONCLUSIONS

In conclusion, the corrugated structures in the diaphragm design can effectively reduce the dependence of the diaphragm stiffness on the residual stress, and proper geometric design of the corrugations can reduce the variations of the tuning characteristics of the diaphragm tuner due to the fabrication uncertainties. With the aid of automated batch mode FEM simulations, a parametric study has been performed to analyze the tradeoff between the pull-in voltage and the tuning range of the capacitive MEMS tuner. Therefore, the diaphragm tuner with low voltage and high tuning ratio can be achieved with special attentions paid to the fabrication

uncertainties. Uncertainty quantification shows that the tuning range varies by ± 5.9% and the actuation voltage varies by ± 9.4% with respect to the a ± 33.3% variation of the residual stress and a ± 9.0% variation of the corrugation depth due to fabrication uncertainties.

REFERENCES

[1] X. Liu, L. Katehi, W. Chappell, and D. Peroulis, High-Q tunable microwave cavity resonators and filters using SOI-based RF MEMS tuners. *Journal of Microelectromechanical Systems*, **19(4)**, 774 – 784, 2010.

[2] M. Arif and D. Peroulis, All-silicon technology for high-Q evanescent mode cavity tunable resonators and filters. *Journal of Microelectromechanical Systems*, **23(3)**, 727 – 739, 2014.

[3] Z. Yang and D. Peroulis, A 23-35 GHz MEMS tunable all-silicon cavity filter with stability characterization up to 140 million cycles. *IEEE MTT-S International Microwave Symposium (IMS)*, Tampa, Florida, June 2014.

[4] E. Naglich, M. Sinani, S. Moon, and D. Peroulis, High-Q MEMS-tunable W-band bandstop resonators. *IEEE MTT-S International Microwave Sympsium (IMS)*, Tampa, Florida, June 2014.

[5] D. Giovanni, *Flat and Corrugated Diaphragm Design Handbook*. CRC Press, 1982.

[6] M. Fuldner, A. Dehe, R. Lerch, Analytical analysis and finite element simulation of advanced membranes for silicon microphones. *IEEE Sensors Journal*, **5(5)**, 857–863, 2005.

[7] ANSYSAcademic Research, Release 14.5, help system, ANSYS mechanical APDL structural analysis, ANSYS, inc, 2014. [Online]. Available: http://ansys.com.

[8] MATLAB, version 7.11.0 (R2010b). Natick, Massachusetts: The MathWorks Inc., 2010.